

## Oriented Attachment: From Natural Crystal Growth to a Materials Engineering Tool

Published as part of the *Accounts of Chemical Research* special issue “*Transformative Inorganic Nanocrystals*”.

Bastiaan B. V. Salzmann,<sup>†</sup> Maaïke M. van der Sluijs,<sup>†</sup> Giuseppe Soligno, and Daniel Vanmaekelbergh\*



Cite This: *Acc. Chem. Res.* 2021, 54, 787–797



Read Online

ACCESS |



Metrics & More

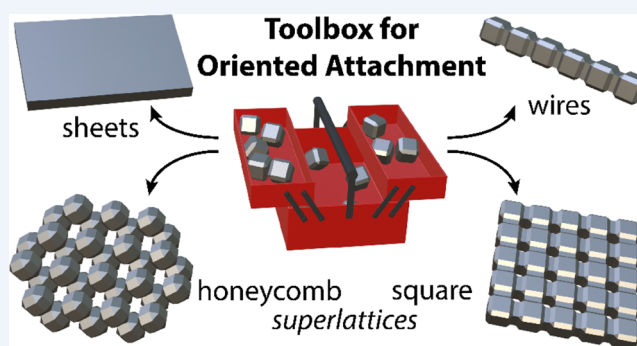


Article Recommendations



Supporting Information

**CONSPECTUS:** Intuitively, chemists see crystals grow atom-by-atom or molecule-by-molecule, very much like a mason builds a wall, brick by brick. It is much more difficult to grasp that small crystals can meet each other in a liquid or at an interface, start to align their crystal lattices and then grow together to form one single crystal. In analogy, that looks more like prefab building. Yet, this is what happens in many occasions and can, with reason, be considered as an alternative mechanism of crystal growth. Oriented attachment is the process in which crystalline colloidal particles align their atomic lattices and grow together into a single crystal. Hence, two aligned crystals become one larger crystal by epitaxy of two specific facets, one of each crystal. If we simply consider the system of two crystals, the unifying attachment reduces the surface energy and results in an overall lower (free) energy of the system. Oriented attachment often occurs with massive numbers of crystals dispersed in a liquid phase, a sol or crystal suspension. In that case, oriented attachment lowers the total free energy of the crystal suspension, predominantly by removal of the nanocrystal/liquid interface area. Accordingly, we should start by considering colloidal suspensions with crystals as the dispersed phase, i.e., “sols”, and discuss the reasons for their thermodynamic (meta)stability and how this stability can be lowered such that oriented attachment can occur as a spontaneous thermodynamic process. Oriented attachment is a process observed both for charge-stabilized crystals in polar solvents and for ligand capped nanocrystal suspensions in nonpolar solvents. In this last system different facets can develop a very different reactivity for oriented attachment. Due to this facet selectivity, crystalline structures with very specific geometries can be grown in one, two, or three dimensions; controlled oriented attachment suddenly becomes a tool for material scientists to grow architectures that cannot be reached by any other means. We will review the work performed with PbSe and CdSe nanocrystals. The entire process, i.e., the assembly of nanocrystals, atomic alignment, and unification by attachment, is a very complex and intriguing process. Researchers have succeeded in monitoring these different steps with in situ wave scattering methods and real-space (S)TEM studies. At the same time coarse-grained molecular dynamics simulations have been used to further study the forces involved in self-assembly and attachment at an interface. We will briefly come back to some of these results in the last sections of this review.



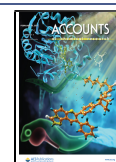
### KEY REFERENCES

1. Boneschanscher, M. P.; Evers, W. H.; Geuchies, J. J.; Altantzis, T.; Goris, B.; Rabouw, F. T.; van Rossum, S. A.; van der Zant, H. S.; Siebbeles, L. D.; Van Tendeloo, G.; Swart, I.; Hilhorst, J.; Petukhov, A. V.; Bals, S.; Vanmaekelbergh, D. Long-range orientation and atomic attachment of nanocrystals in 2D honeycomb superlattices. *Science* 2014, 344, 1377–1380.<sup>1</sup> Two-dimensional honeycomb superlattices are prepared by oriented attachment of PbSe nanocrystals. Direct imaging and wave scattering methods reveal that the superlattices are atomically coherent and have a buckled octahedral symmetry.

2. Geuchies, J. J.; van Overbeek, C.; Evers, W. H.; Goris, B.; de Backer, A.; Gantapara, A. P.; Rabouw, F. T.; Hilhorst, J.; Peters, J. L.; Konovalov, O.; Petukhov, A. V.; Dijkstra, M.; Siebbeles, L. D. A.; van Aert, S.; Bals, S.; Vanmaekelbergh, D. In situ study of the formation mechanism of two-dimensional superlattices from PbSe nanocrystals. *Nat. Mater.* 2016, 15, 1248–1254.<sup>2</sup> *The*

Received: November 12, 2020

Published: January 27, 2021



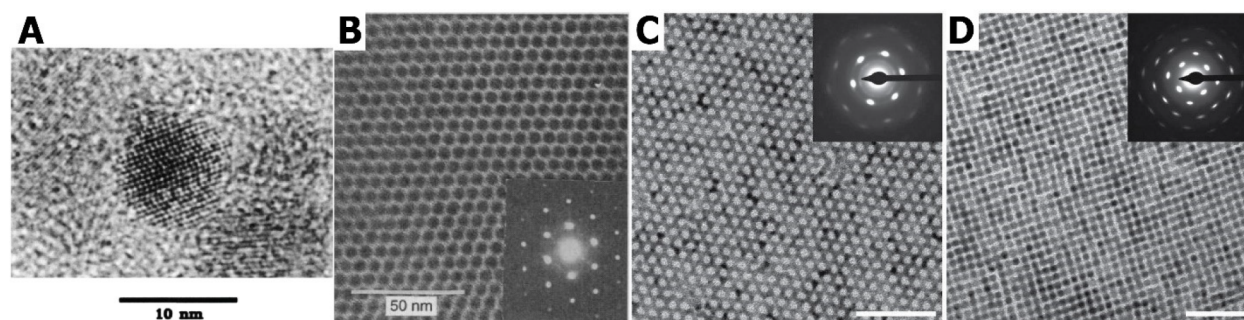


**Figure 1.** From single building blocks to superlattices prepared via oriented attachment. High-resolution TEM image of a single CdSe quantum dot (A) which can be self-assembled into a superlattice in which the nanocrystals are ordered although not connected (B). Panel A reproduced with permission from ref 8. Copyright 1993 American Chemical Society. Panel B reproduced with permission from ref 28. Copyright 1995 AAAS. In the case of PbSe nanocrystals, further modification of the reaction conditions results in the formation of nanocrystals attached via the (100) facets, resulting in either honeycomb (C) or square superlattices (D). Scale bar represents 50 nm and insets show SAED patterns, indicating the high crystallinity of the formed structures. Panels C and D reproduced with permission from ref 43. Copyright 2013 American Chemical Society.

*formation mechanism of PbSe square superlattices was revealed by combining wave scattering techniques with electron microscopy and Monte Carlo simulations. We observe different intermediate stages and final attachment of the nanocrystals at the (100) planes.*

- Peters, J. L.; Altantzis, T.; Lobato, I.; Jazi, M. A.; van Overbeek, C.; Bals, S.; Vanmaekelbergh, D.; Sinai, S. B. Mono- and Multilayer Silicene-Type Honeycomb Lattices by Oriented Attachment of PbSe Nanocrystals: Synthesis, Structural Characterization, and Analysis of the Disorder. *Chem. Mater.* **2018**, *30*, 4831–4837.<sup>3</sup> *Large-scale uniform mono- and multilayer silicene-type honeycomb PbSe superlattices are prepared by oriented attachment. Different classes of disorder in the lattices are explained in terms of position and atomic alignment of the nanocrystals.*

## 1. SUSPENSIONS WITH (NANO)CRYSTALS AS DISPERSED PHASE

We discuss systems in which crystalline solid particles are dispersed in a continuous liquid medium, hence the specific case of a “sol”. The colloidal particles have dimensions between 1 and 1000 nm, thus from a few unit cells to several thousands in one direction. Such sols can remain stable as a two-phase system for years: their (meta)stable state corresponds to a (local) minimum in the free energy. To understand the microscopic origin of colloidal stability, we have to distinguish crystal suspensions in water or other polar solvents from suspensions in organic apolar media, such as, e.g., hexane or toluene.

### Charge-Stabilized Suspensions

Suspensions of inorganic crystals in water are stabilized against agglomeration by a double layer of charges: positive or negative ions at the surface of the crystals and an equal amount of counter charge present in the diffuse part of the double layer.<sup>4</sup> The width of this charge double layer is dependent on the concentration of ions in the medium, allowing for a subtle engineering of repulsion and attraction between the particles.<sup>5</sup> Oriented attachment between inorganic crystals in water is observed in natural biological conditions and is assumed to be important for biomineral formation. Commonly, crystal growth by oriented attachment is coined nonclassical crystal growth,<sup>6,7</sup> to distinguish it from the classical atom-by-atom (molecule-by-molecule) growth of crystals. In oriented attachment,

attractions between specific facets are dominant and when facets connect, the crystal surface energy is reduced. Oriented attachment thus lowers the enthalpy of the system in a thermodynamic *spontaneous* process. A further review of attachment in polar solvents can be found in the [Supporting Information](#).

### Sterically Stabilized Nanocrystals Dispersed in an Organic Phase

In the rise of colloidal nanoscience that started around 1985, a second type of sol became very prominent, namely, that in which crystals with dimensions in the 1–20 nm range (thus nanocrystals, NCs) are dispersed in nonpolar organic solvents.<sup>8</sup> The nanocrystals are sterically stabilized against aggregation by organic ligand molecules bound with a chemical functionality to the nanocrystal surface and have an alkyl chain immersed in the liquid. The interaction between the ligands of two adjacent nanocrystals is very similar to the interaction between the ligands and the solvent molecules. As a consequence, the ligand–ligand attraction is screened by the “ideal” solvent; the only attractive interaction is then the van der Waals type attraction between the nanocrystal cores on a distance defined by the two ligand layers.<sup>9,10</sup> For sufficiently small nanocrystals, the attractions constitute an energy in the order of the thermal energy, weak enough to keep such suspensions stable. To initiate colloidal crystallization, the system has to be destabilized. This is possible by making the solvent less “ideal”, for example by adding a polar nonsolvent.<sup>9,11</sup> To initiate oriented attachment, the attraction between specific facets has to be increased, e.g., by replacing the ligands bound to a specific type of facet with a smaller surface-active species or by desorption of the ligands from a specific facet due to the presence of a second liquid phase with a high affinity for the ligands. The binding strength of the ligands on the facets, and the ligand density depends on the atomic structure of the facet in question.<sup>12–14</sup> Running ahead on what comes, we provide here the example of truncated cubic PbSe crystals; oleate ligands are only weakly bound to the 6 (100) facets, while the (110) and polar (111) facets are firmly covered with these ligands. In 2005 it was found that oriented attachment by (100) facet-to-facet connection can result in highly anisotropic PbSe rods, with their long axis being  $\langle 100 \rangle$ .<sup>15</sup> But with other ligands (or amines) the reactivity of the facets can be changed and oriented attachment could be achieved involving exclusively the (110) or (111) facets.<sup>15,16</sup> The exclusiveness

of only one facet type being active in oriented attachment is remarkable, and more pronounced for organic sols, than for aqueous suspensions.

## 2. BRIEF HISTORY OF ORIENTED ATTACHMENT IN NONPOLAR ORGANIC SOLVENTS

### General History

In the early 1990s, wet chemical methods using precursors and ligands soluble in organic solvents were developed to prepare nanocrystals of semiconductor compounds.<sup>17,18</sup> Exemplary for this development is the publication in 1993 by Murray, Norris, and Bawendi on CdSe nanocrystals of 1–10 nm in diameter;<sup>8</sup> see Figure 1A. In this work the nanocrystals were capped with organic ligands which bind to the surface Cd atoms and dispersed in an organic solvent. Due to the favorable interactions between the solvent and the alkyl chains, such dispersions are sterically stabilized. Upon optical excitation, an (e,h) exciton eigenstate was formed that recombined radiatively. Both the absorption and luminescence spectra showed that the exciton was strongly confined in the nanocrystal. Hence, by changing the size of the nanocrystals the emission color could be tuned over a wide energy range. Further research resulted in development of nanocrystals of other II–VI, III–V, and IV–VI compounds synthesized with similar methods.<sup>19</sup> Nanocrystals of the IV–VI compounds, especially the PbX family (X = S, Se, Te), were extensively investigated as their band gap spans the near IR and can, again, be tuned by the degree of exciton confinement. Over three decades these interesting properties have led to an explosion of fundamental and applied research, and to innovative optoelectronic applications.<sup>20–24</sup>

### Oriented Attachment as a New Tool in Nanomaterials Science

The synthesis of semiconductor nanocrystals with hot-injection techniques has had a tremendous effect on fundamental nanocrystal science and its applications. The surface passivation by organic and inorganic ligands resulted in electronic passivation, such that electronic and excitonic eigenstates instead of surface trapped states become fully visible in spectroscopy. This opened the gate to fundamental studies of the electron energy levels and exciton dynamics of semiconductor nanocrystals with a plethora of optical spectroscopic techniques and electron tunneling spectroscopy.<sup>25,26</sup> Electrons, holes, and electron–hole pairs have a wave nature, and when they are confined in nanocrystals, they experience a quantum confinement effect that increases their kinetic energy. Hence, the single-electron energy levels and exciton energies in nanocrystals are strongly size dependent. This, and the strongly radiative emission, boosted the scientific interest in semiconductor nanocrystals. It has resulted in large-scale applications using well-defined CdSe and InP nanocrystals as spectral converters in displays and TV screens.<sup>24</sup>

### Driving Forces and Facet Specificity in Oriented Attachment

Nanocrystals prepared by hot-injection methods in organic solvents can have a well-defined crystal structure and shape and are terminated by facets with a specific surface chemistry and energy. As a consequence, the binding energy and density of the ligand molecules on specific facets differs considerably. Hence, oriented attachment of organic-capped crystals is facet-specific in a more pronounced way than for charge-stabilized

nanocrystals. At the same time the shape of the nanocrystals is influenced by the capping density of the facets. For instance, a well-capped PbSe nanocrystal has the shape of truncated octahedron, but if the ligand density is lowered by washing, the shape changes toward that of a truncated cube.<sup>27</sup> Therefore, PbSe nanocrystals with a simple rock salt structure provide the best example to illustrate the pronounced facet specificity in oriented attachment.

### Colloidal Crystallization, Formation of Superlattices

Suspensions of semiconductor nanocrystals in good organic solvents are well-stabilized against aggregation and can thus be prepared in highly concentrated suspensions. In these suspensions the ligand–ligand interactions are screened by the solvent molecules, and the semiconductor core–core attractions are small.<sup>9,10</sup> Only for larger crystals, rods, and metallic crystals, the attractions between the nanocrystals start to increase to a few times the thermal energy at room temperature. The colloidal crystallization of these nanocrystals from suspensions became a matter of interest around 1995.<sup>28</sup> Since nanocrystal suspensions are stable, the suspension can be destabilized in a subtle way; in other words, *colloidal crystal engineering with the formation of well-ordered superlattices is possible*. An example of this can be seen in Figure 1B. From a nanoscience materials perspective, truly new material platforms emerged, since nanocrystal assembly is the only way to bring nanoscale building blocks in close contact in an ordered structure.<sup>29,30</sup> The superstructures formed by increased concentration in the suspension can be seen as a hard-sphere framework forming a face-centered-cubic structure (fcc). In contrast, by adding a more polar but miscible component, the solvent medium becomes less ideal and colloidal crystallization driven by the nanocrystal attractions (ligands and cores) occurs. At a lower ligand density the interactions become more soft-sphere-like, and the resulting structures are body-centered tetragonal (bct) or even body-centered cubic (bcc).<sup>31,32</sup> However, the organic ligands still present tend to form a tunneling barrier for the charge carriers, resulting in weak electronic coupling and carrier mobilities substantially below 1 cm<sup>2</sup>/(V s).<sup>33–35</sup> Coupling between the nanocrystals could be improved by exchanging the long organic ligands for shorter ones,<sup>36,37</sup> or by exchanging for ligands that specifically couple the nanocrystals, or exchanging for ligands that change the band alignment between different quantum dots from type-I to type-II.<sup>38,39</sup> With this advanced engineering, reasonable carrier mobilities of 0.1–20 cm<sup>2</sup>/(V s) have been reached in NC solids.<sup>36,40–42</sup>

A considerable increase in carrier mobility could, in principle, be achieved by oriented attachment, which ideally results in a crystalline neck between the nanocrystals in a self-assembled structure. The coupling is then only limited by the width of the neck. Below, we will discuss the formation of 2D superlattices consisting of a monolayer of nanocrystals that are epitaxially connected. In the case of PbSe (and PbS, PbTe) atomically coherent superlattices could be prepared<sup>1–3,43–45</sup> that have a square geometry (thus also with a square periodicity of voids) and a honeycomb geometry (hexagonal periodicity of voids); see Figure 1C,D. It was shown that the electronic band structure of square and honeycomb superlattices was different from the simple 2D sheets or quantum wells prepared by oriented attachment.<sup>16</sup> Honeycomb semiconductors show a conventional band gap, but the electron conduction bands (hole valence bands) show Dirac-type



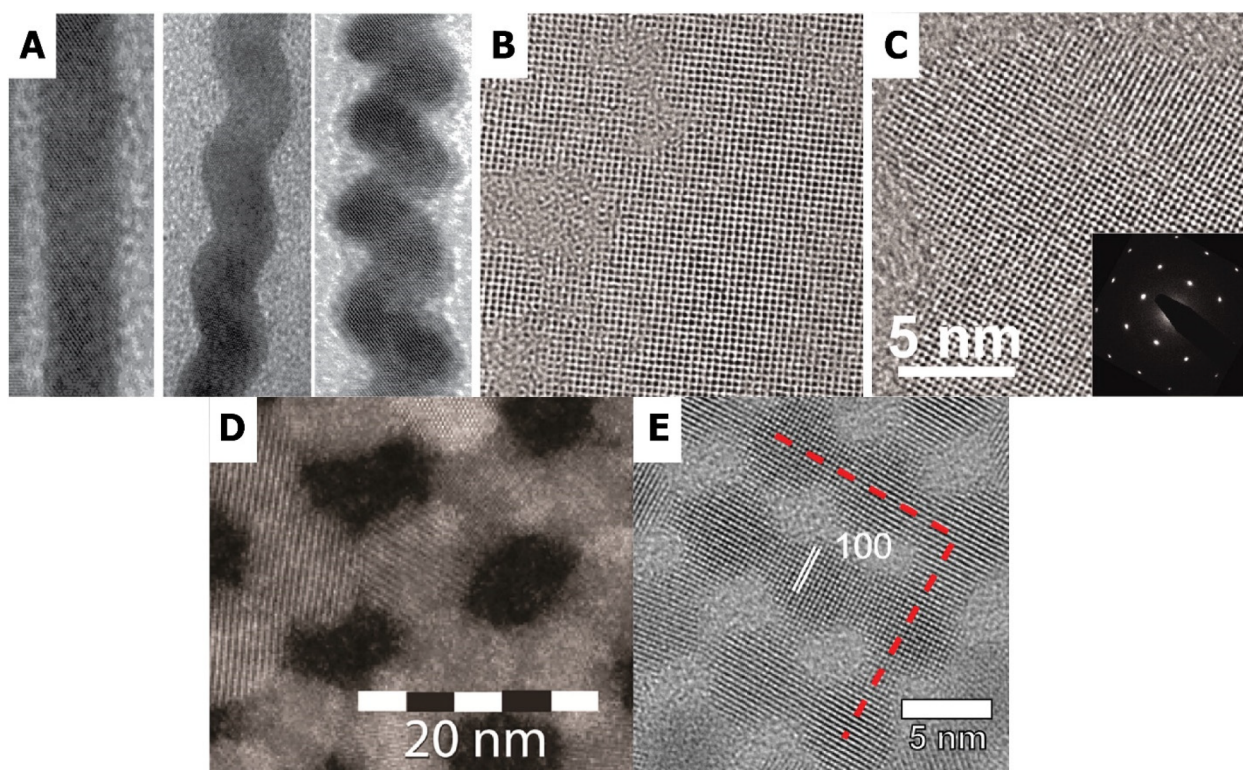


**Figure 2.** Oriented attachment of lead chalcogenide nanocrystals resulting in a variety of nanostructured materials. Depending on the reaction conditions, oriented attachment of PbSe nanocrystals lead to 1D single-crystal wires (A) which are either straight (left) or zigzag (middle and right). Panel A reproduced with permission from ref 15. Copyright 2005 American Chemical Society. Alternatively, 2D sheets can be prepared by selective attachment of (110) facets. In an early stage, small holes are visible in the crystal structure (B), whereas at a later stage single crystalline particles are obtained (C), confirmed with SAED (inset). Panels B and C reproduced with permission from ref 16. Copyright 2010 AAAS. Oriented attachment of presynthesized PbS nanocrystals can result in either square or honeycomb superlattices by attaching at (100) facets; corresponding high-resolution HAADF-STEM images are shown in (D) and (E). Panels D and E respectively reproduced with permission from refs 27 and 59. Copyright 2017 and 2016 American Chemical Society.

bands, similar to those of graphene!<sup>46,47</sup> This brings the exciting opportunity to combine typical semiconductor properties with electron and hole excitations that are “massless” as in graphene. So far, experimental evidence for these compelling predictions has not been found, as the electronic mobilities are relatively low (1–10 cm<sup>2</sup>/(V s)), being limited by imperfect necks and geometrical disorder.<sup>48–50</sup> However, the big message here is that the electronic band structure of 2D crystals can be engineered by the lateral nanogeometry of the system.<sup>51</sup> Specific geometries can be achieved by NC assembly followed by oriented attachment. The big challenge in this very promising field is to grow 2D structures using identical nanocrystal building blocks, resulting in 2D superstructures without geometrical disorder and with uniform necks.<sup>52,53</sup>

### 3. ORIENTED ATTACHMENT IN THE FAMILY OF PBX NANOCRYSTALS, WITH PBSE NCS AS LEADING EXAMPLE

#### Formation of Highly Anisotropic 1D and 2D Crystals in the Rock Salt Family

In a one-pot synthesis of PbSe nanocrystals using limited amounts of oleate ligands, PbSe nanorods and long nanowires (up to 30 μm in length and 4–20 nm in diameter) can be formed along the ⟨100⟩ direction;<sup>15,54,55</sup> see also Figure 2A. It is hypothesized that nanocubes are formed first, which act as intermediates that attach via their (100) facets. Since there are

six (100) facets in the three orthogonal directions, one expects the formation of 3D superlattices. Nevertheless, strong anisotropic one-dimensional (1D) structures are observed, built from centrosymmetric rock salt nanocrystals.<sup>15</sup> An explanation on the basis of NC dipoles has been proposed, but independent information on the existence of an electric dipole in PbSe NCs is lacking.<sup>56</sup> In the case of rock salt PbSe, usually the low-energy (100) facets are active in oriented attachment, as they are most easily liberated from the oleate ligand molecules.<sup>57,58</sup> However, when amines are applied in the one-pot synthesis, used to exchange the oleate capping on existing nanocrystals or when a cosolvent is added, novel 1D rods, wires, and sheets are observed that can only be understood by exclusive (110)/(110), or even (111)/(111), facet-to-facet attachment.<sup>15</sup> Hence, in some cases specific ligand capping can alter the relative reactivity of the facets for oriented attachment. Later on, a *one-step* method was developed for the preparation 2D PbS sheets;<sup>16</sup> see Figure 2B,C. Here, the nucleation and growth of PbS nanocrystals are followed by oriented attachment at (110) facets in two directions due to the addition of a chlorine-containing cosolvent. The resulting well-defined PbS quantum wells have a thickness of about 4 nm and showed photoconductivity.

#### Formation of 2D Atomically Coherent Superlattices with a Square or Honeycomb Geometry

The formation of atomically coherent superlattices with a square and a honeycomb geometry by NC assembly and



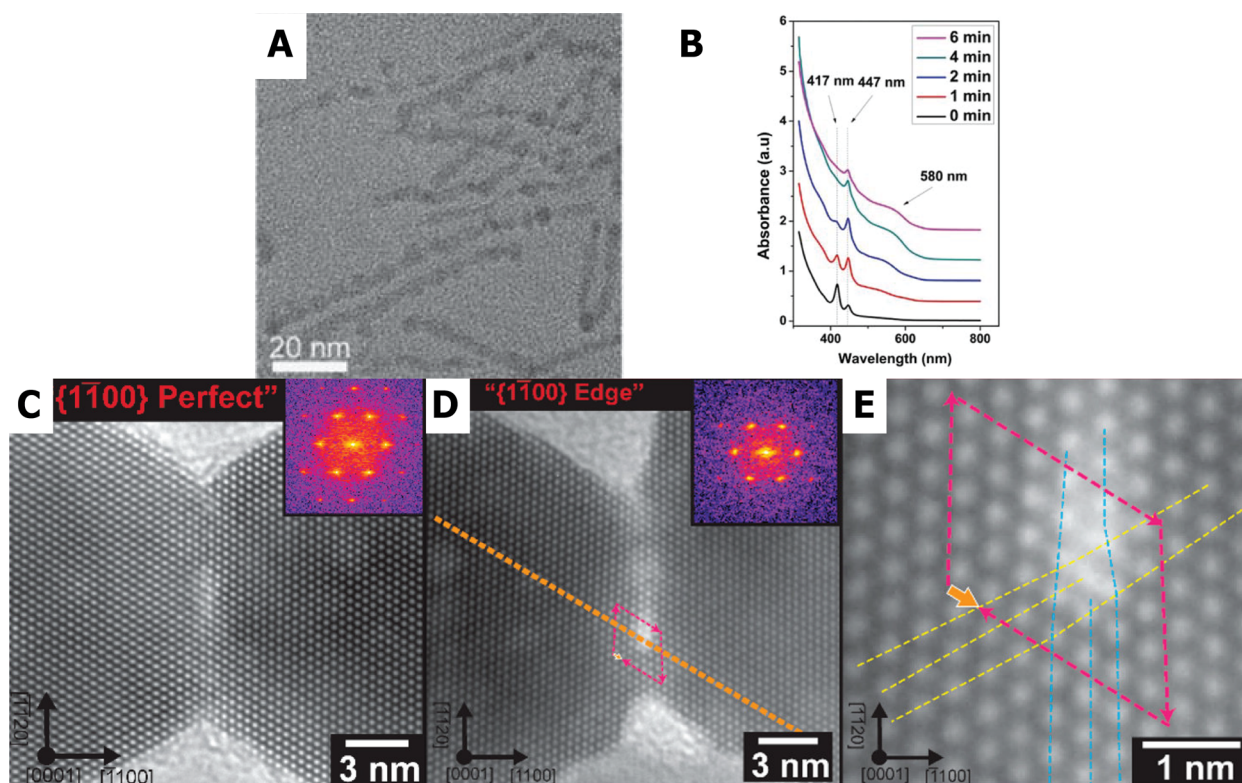


**Figure 3.** Oriented attachment of cadmium chalcogenide nanocrystals. The formation of pearl necklaces, composed of small nanocrystals, is clearly visible due to the different thicknesses in a single wire and is strong proof for oriented attachment of smaller nanocrystals (A). In several cases, magic-sized clusters have been observed as intermediates during the formation of these wires (B). In here, characteristic absorption features at 417 and 447 nm appear and disappear during the preparation. Panels A and B reproduced with permission from ref 67 Copyright 2015 American Scientific Publishers. In situ TEM shows the absence (C) or presence (D) of defects between two CdS nanocrystals. High-resolution imaging (E) enables the study of local defects. Panels C–E reproduced with permission from ref 68. Copyright 2019 American Chemical Society.

oriented attachment came to us as a big surprise. In 2012 we were performing experiments on the self-assembly of PbSe NCs in the framework of understanding the interactions between the nanocrystals. PbSe NC suspensions were drop-cast on ethylene glycol (EG), which we considered at the time as an inert liquid substrate. With additional oleate present, simple monolayers (bilayers) with hexagonal ordering of NCs were formed. However, if the nanocrystals were well-washed, we observed different geometries (Figure 2D,E): we found monolayers in which the NCs were organized in square arrays, also showing a square array of voids due to the truncation of the cubic shape of the NCs. Alternatively, we observed 2D systems, with a hexagonal array of voids, which means that the semiconductor material structure must have the honeycomb geometry. Often domains with square and honeycomb geometry were found together. Most interestingly, we found that, in both cases, the PbSe NCs were attached via the (100) facets, with four connections in the case of the square superlattice, and three connections in the case of the honeycomb lattice. Clearly, the ligand density of the (100) facets reduced due to the washing step, but very probably also due to EG liquid interface. While the (100)/(100) connection is simple to understand for the square geometry, for the honeycomb geometry we realized that the (100) connections also imply that the nanocrystals are aligned with the (111) axis upward and that the honeycomb is buckled, unlike graphene, but very similar to silicene and germanene.<sup>1,3</sup>

The formation of PbSe superlattices with a honeycomb geometry is surely the most intriguing process of oriented

attachment so far. It is also the most difficult to reproduce in many respects. It was found that very slow evaporation of the suspension solvent (usually toluene) over 15 h and lowering of the (100) facets reactivity, e.g., by adding 1,4-butanol to the liquid substrate, can result in well-ordered and large domains.<sup>3</sup> The system can be so well-ordered that point defects and line defects in the structure become visible as in classic crystallography. An example of this is presented in Figure 2D. The formation of square and honeycomb structures is a complex process, with several consecutive phases. It is clear that the nanocrystals should be able to align in a reversible way, thus before irreversible epitaxial connections are formed. The question of which forces drive the alignment of the nanocrystals, before they attach and form an atomically coherent structure, is an interesting one. The orientation of nanocrystals at the air/toluene interface has been put forward,<sup>60–64</sup> as well as the chemical attraction between bare (100) facets. The evolution of the entire process has been monitored in situ with synchrotron radiation and ex situ electron microscopy, which will be discussed in Section 5. As this interfacial assembly and oriented attachment opened the gate to truly novel material classes (see above), our initial experiments were extended by beautiful efforts of several other groups.

In an effort by a group in Ghent, the formation of the epitaxial connection was triggered by addition of amines or Na<sub>2</sub>S to the liquid substrate. This resulted in the formation of square lattices in a short time, with lattice domain sizes of about 100 nm (15–20 nanocrystal unit cells); see Figure 2E.

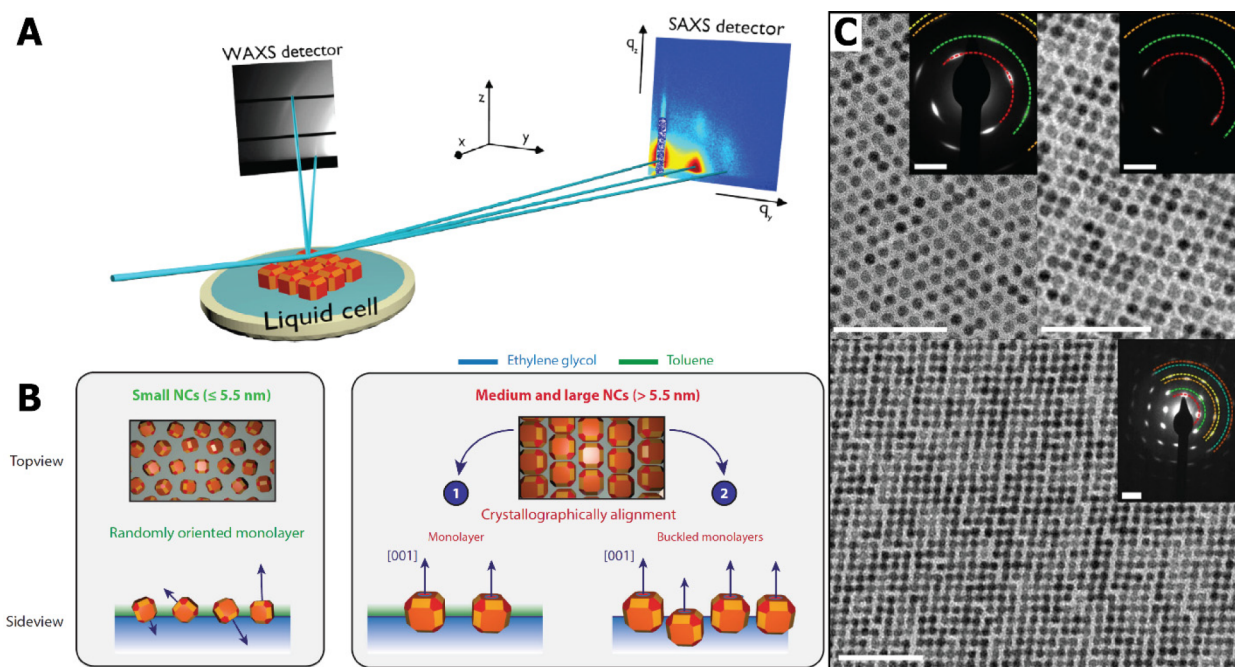


**Figure 4.** Schematic setup used for in situ grazing incidence X-ray scattering experiments (A). The solvent from a NC dispersion evaporated in a liquid cell, placed in a chamber (not depicted). The assembly and attachment are studied by simultaneously monitoring atomic ordering on the wide-angle detector (WAXS) and nanoscale ordering on the small-angle detector (SAXS). Schematic representation of the orientation of nanoparticles at the ethylene glycol–air interface based on in situ scattering experiments (B). Small NCs are randomly oriented, while larger particles (5.5–9 nm) have a more cubic shape, with larger (100) facets of which one aligns favorably perpendicular to the interface. Panel B reproduced with permission from ref 74. (C) TEM images from samples taken during in situ experiments. They show a pseudo-hexagonal phase (top left), an initial square phase (top right) before complete attachment, and the final square phase (bottom); the scale bars correspond to 50 nm. The inset shows ED patterns which transform from arcs to distinct spots. Panels A and C reproduced with permission from ref 2. Copyright 2016 Nature.

These chemical triggers were chosen on the basis of the idea that interdot connections can only form between (100) facets which face each other and have a *stoichiometric surface*; then  $S^{2-}$  adds sulfur to a (100) surface with Pb excess, while amines pull excess lead ions away. After addition of these chemical triggers, it takes only 5 min for the epitaxially connected superlattice to form domains of  $\sim 100$  nm in size. With the amine trigger the basicity can be tuned, resulting in a more gentle ligand displacement with a weaker base, which appears to increase the domain size of the superlattice.<sup>59</sup>

The formation of 2D square and honeycomb superlattices, and straight and zigzag 1D structures as well, is not limited to PbSe NCs; formation of these structures also occurs with PbS and PbTe nanocrystals.<sup>45</sup> The studies so far are very limited, but it is justified to say that PbTe NCs are the most reactive PbX system. Therefore, the attachment is challenging to control, and it is difficult to obtain ordered structures with a reasonable domain size.

#### 4. ORIENTED ATTACHMENT IN THE CDX NANOCRYSTAL FAMILY

The family of CdX nanocrystals ( $X = S, Se, Te$ ), with CdSe here as the dominant example, have a relatively rigid lattice due to covalent bonding. This means that the nanocrystals are not so easily reshaped as those from the PbX family and thus show less propensity for oriented attachment. Still, there is strong evidence that oriented attachment (or a process like this) occurs during the preparation of wires and sheets; there are multiple reports on the attachment of mature NCs or small magic-size clusters, which we will discuss below. Compared to

the rock salt PbX family, oriented attachment of CdX nanocrystals is more difficult to study as both wurtzite (hexagonal and polar along the  $c$ -axis) and zinc blende (cubic and isotropic) NCs with very different chemistry and polarity of the facets can play a role.

#### Growth of CdX Nanowires: A Case of Oriented Attachment?

Tang et al. revealed that wurtzite CdTe nanowires could be grown via the attachment of smaller zinc blende nanocrystals.<sup>65</sup> Epitaxial connections were achieved by controlled removal of ligands from the nanocrystals' surface. Aliquots taken at short reaction times showed pearl-necklace aggregates which evolve to wires with aspect ratios up to 500. The final CdTe nanowires have the same diameter as the original nanocrystal building blocks which supports oriented attachment as the growth method. Dipole–dipole interactions between the nanocrystals were invoked as the driving force for the attachment process. The observation of nanowire photoluminescence confirmed the single crystalline nature of the wires and a reasonable electronic passivation of the surface.

#### Nanocrystals Formed by “Attachment” of Magic-Size Clusters

We have put attachment between quotation marks: magic-size clusters (MSCs) have a well-defined structure, but without genuine periodicity and crystal facets. Hence, if magic-size clusters unify, and a nanocrystal is eventually formed, atomic reconfigurations must have occurred which go beyond the formation of necks. By reacting cadmium oleate and selenourea with amines at relatively low temperature, CdSe nanowires can



be prepared out of magic-sized clusters.<sup>66</sup> In the first stage, these clusters are formed, which attach and yield precursors aggregates (also called “pearl necklaces”). Subsequent annealing converts these structures into single crystalline wurtzite wires. Later work by Liu et al. showed the preparation of zinc blende CdSe wires via attachment of CdSe magic-size clusters (Figure 3A).<sup>67</sup> Absorption spectroscopy of aliquots showed the formation and disappearance of a magic-sized cluster composed of (CdSe)<sub>33</sub> and (CdSe)<sub>45</sub>, absorbing at 417 nm, which consequently unifies into larger magic-size clusters absorbing at 447 nm; see Figure 3B. More importantly, during further evolution of the reaction, the signatures of the magic-size clusters disappear and absorption of a broad band emerges around 580 nm, signaling the formation of CdSe nanowires. Due to the emergence of an electrical dipole of increasing magnitude along the [111] direction, the attachment of new MSCs is accelerated.

### Formation of 2D Sheets and Quantum Wells by Oriented Attachment

Oriented attachment of CdTe nanocrystals capped with aminothiols resulted in monolayers of attached NC building blocks with lateral extension up to several micrometers.<sup>69</sup> The experimental results, combined with molecular simulations, indicated that in addition to dipole–dipole interactions, small positive charges, and hydrophobic interactions between the nanocrystals are required driving forces for the self-assembly process.

### Investigating the Attachment of Single Nanocrystals

Ondry et al. studied the attachment of two wurtzite CdSe nanocrystals and the removal of defected connections in the presence of an electron beam during in situ TEM.<sup>68</sup> Upon treating the sample with Na<sub>2</sub>Se, the ligands were removed and the nanocrystals attached via their (1100) or (1120) side facets; see Figure 3C. It was found that the formation of epitaxial connections between the crystals comes with crystal dislocations due to the presence of half-finished planes at a facet; an example of this is shown in Figure 3D,E. In some cases, annealing induced by the electron beam allowed removal of the crystal dislocation; its gradual shift toward the surface and “escape” could be followed in situ.

## 5. IN SITU MONITORING OF ORIENTED ATTACHMENT WITH SCATTERING METHODS

Transmission electron microscopy (TEM) has given great insight into the structure and order of superlattices, but it is limited to the in situ study of attachment on a very small scale<sup>68,70</sup> or the study of an already formed superlattice on the larger scale. The only way to study the attachment process with TEM is by samples taken during formation that are immediately dried to be studied later.<sup>3,71</sup> Alternatively, the fast temporal resolution (200 ms) of synchrotron-based specialized X-ray scattering techniques is a strong tool for the study of large-scale superlattice formation. As superlattices are formed on a liquid interface, a grazing incidence (GI) geometry setup is used; see Figure 4A. Instead of transmission scattering, the collimated X-ray beam is bent down toward the liquid surface to scatter the superlattice. The technique is especially interesting as superlattices are crystalline on both the nanocrystal and the atomic length scales. At wide scattering angles, the signal consists of the atomic form factor (scattering strength of the atoms) and the structure factor (positions of the atoms in the unit cell). At small scattering angles, the signal

consists of the form factor from the nanocrystal size and shape and the structure factor from the position of the nanocrystals. Combining these techniques with a chamber allows these experiments to be performed in an inert atmosphere where the solvent–vapor pressure can be regulated, allowing for in situ study of the formation under different conditions.<sup>31,72,73</sup>

Interest has shifted to the study of the different steps observed in the attachment of a monolayer of nanocrystals. Using synchrotron-based in situ GISAXS, the initial spread of a PbSe NC dispersion (6 nm particles) on the liquid substrate (EG) was studied. With remote control, 1  $\mu$ L of a concentrated dispersion was drop-cast  $\sim$ 1.5 cm from the beam, allowing the droplet spreading to be captured (taking  $\sim$ 30 s). Weak Bragg peaks are observed in the GISAXS immediately after drop-casting, suggesting a “precursor film” spreading quickly ahead of the bulk droplet, a phenomenon known in classical wetting theory as a “molecular” film bridging the interfacial energy discontinuity at the contact line.<sup>75</sup> Within the first 2–5 s the bulk droplet follows, and as the solvent evaporates the nanocrystal concentration in the film gradually increases. A phase transition to a dense liquid, and then a network of solvated but correlated quantum dots, is observed. When at last (after  $\sim$ 26 s) all of the solvent has evaporated, strong scattering rods are observed, resulting in an fcc-like superstructure. However, the simultaneous GIWAXS measurements show only rings, indicating no preferential orientation of the NCs at these time scales.<sup>76</sup> However, more recent experiments showed that in the presence of additional oleate ligands crystallographic alignment is observed. After 2 h of evaporation, medium and large NCs (5.5–9 nm) showed orientation with the [100] axis perpendicular to the liquid/air interface; see Figure 4B.<sup>74</sup>

In attachment experiments on longer time scales (evaporation of 1 h), the formation mechanism of 2D PbSe superlattices with square geometry was observed. In these experiments GISAXS/GIWAXS was combined with ex situ TEM and electron diffraction to elucidate the phase transfers. After drop-casting 350  $\mu$ L of a dilute dispersion of  $\sim$ 5.7 nm PbSe NCs, Bragg peaks are observed at the EG interface after 16 min, indicating the presence of a hexagonal monolayer. Hard-sphere interaction still dominates the particle interaction at this point. However, in another 15 min, it transforms via a pseudo-hexagonal phase (bond angles deviating from 60°) to a phase with square ordering (bond angles of 90°); see Figure 4C. These phase transitions are interpreted as increasing NC attractions, as ligands gradually strip from the lower energy (100) facets and square ordering of the structure is driven to maximize facet overlap. During this transformation, the orientational freedom of the NCs also decreases gradually (bands in the GIWAXS), until the NCs attach via necks (spots in the GIWAXS). The resulting square superlattice has a NC–NC distance of 7.6 nm, which is 34% larger than the original PbSe NC core diameter, and an average atomic coherence length of 13.2 nm, again indicating attachment of the quantum dots to on average a lower limit of two to three NC diameters.<sup>2</sup>

## 6. MOLECULAR DYNAMICS SIMULATIONS OF NANOCRYSTAL ASSEMBLY AND ATOMIC ALIGNMENT AT AN INTERFACE

Despite efforts to develop a predictive theoretical framework for modeling crystallization by oriented attachment,<sup>77</sup> the observation of remarkable 2D superstructures with a square or silicene-type honeycomb geometry on the length scale of the

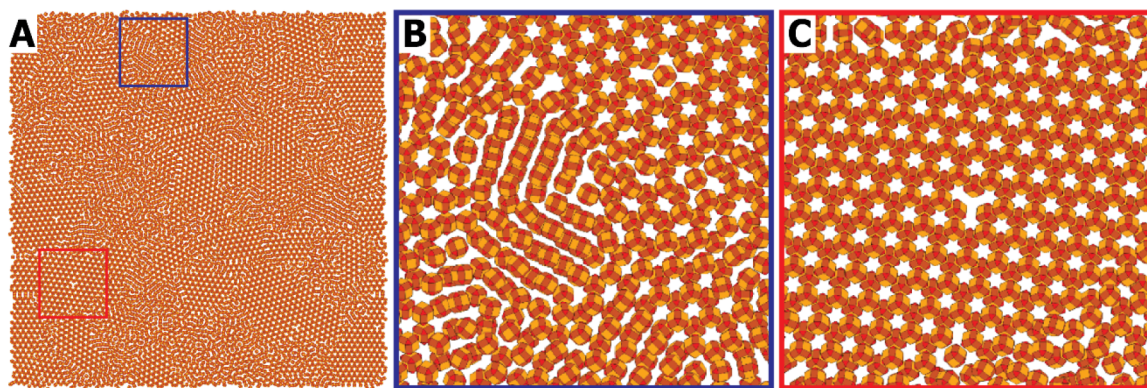


**Figure 5.** Molecular dynamics simulation of the self-assembly and oriented attachment of nanocrystals with a truncated cubic shape, presented by a still taken after 0.15  $\mu\text{s}$  of simulation. (A) Overview of a simulation with 10000 nanocrystals, showing crystalline domains of the honeycomb phase together with amorphous (disordered) parts; (B) detailed picture showing zigzag linear structures that were not able to organize into the honeycomb lattice; (C) detail with a crystalline-like vacancy defect in the honeycomb structure.

nanocrystals (roughly 10 nm) showing epitaxial connections between the nanocrystals raises many intriguing questions. To date, these questions are still not fully resolved. Intuitively, the formation of 2D structures points to nanocrystals that absorb at an interface; the results of in situ synchrotron experiments described above suggests that this could be the liquid/air interface. On the other hand, it could also be that nanocrystals form a thin film within a thin layer of organic solvent at the end of the solvent evaporation process. By intuition again, the formation of large NC systems (sometimes thousands of unit cells) with nanoscale order and alignment suggests that the process of irreversible oriented attachment (crystal necking) is relatively slow and that ordered and aligned phases of many NCs form. The big question that rises is then, what types of forces are responsible for the alignment of the cubic PbSe nanocrystals?

Realistic course-grained molecular dynamic simulations (MD simulations) have been carried out in our group in order to resolve these questions and, more generally, to get an answer to whether large phases of aligned nanocrystals can form spontaneously without epitaxial connections. In coarse-grained models, atomic-scale details are sacrificed, but features such as size, shape, and softness of the NCs—which can be modeled on a larger scale than the atomic one—are retained, allowing simulations in the order of 10000 NCs.<sup>78</sup> Soligno and Vanmaekelbergh<sup>62,63</sup> calculated the free energy change of nanocrystal adsorption at the toluene/air interface. It was found that the free energy change of adsorption is many times the thermal energy, indicating that a 2D layer of nanocrystals can form at an interface. For PbSe nanocrystals with a truncated cubic shape it was observed that the adsorption geometry with a vertical (100) or (111) axis is favored with respect to other orientations. Hence, oriented nanocrystal adsorption may, in principle, result in a partial alignment of the crystals at the interface, although there is a remaining rotational degree of freedom in the plane of the interface. Realistic MD simulations were carried out, accounting for attractive and repulsive interactions between the nanocrystals, entropic effects, and forces due to capillary deformations of the solvent/liquid interface. It was convincingly shown that both square superlattices and silicene honeycomb lattices could arise from NCs adsorbed at the toluene/air interface. Recently, these simulations have been extended to phases consisting of as much as  $10^4$  nanocrystals, with a further relaxation of the

boundary conditions by allowing no preferential absorption at an interface at time  $t = 0$ . A still of the MD simulations is shown in Figure 5. Again, honeycomb lattices and linear structures were observed after a certain simulation time. Moreover, the natures of the disorder in these phases, consisting of small superlattice domains, linear NC structures, linear zigzag structures, and very remarkable vacancies, were all present in the simulations, very similar to how they were observed in a large number of TEM analyses of samples from experiments. Although MD simulations can successfully reproduce the experimentally observed superlattices and the disorder that arises in them, the question of which forces are key for the nanocrystal alignment (interfacial adsorption, entropic ordering of hard cubes, or (100)/(100) facet/facet attractions) is not fully answered yet. The enigma of the beautiful honeycomb silicene superlattices with ordering over hundreds of unit cells, which has been observed on several occasions, is not yet fully resolved.

## 7. SUMMARY AND OUTLOOK

Oriented attachment, the unification of two separate crystals to form one single crystal, was once not much more than a curiosity, based on a number of observations in biological mineral formation and geology. However, it became known as “non-classical” crystal growth and got a complementary place next to the atom-by-atom, row-by-row, or plane-by-plane crystal growth that has been observed and modeled in classic crystallography. The new age of nanocrystal synthesis in nonpolar organic solvents, starting at the beginning of the 1990s, provided a new and compelling chapter to oriented attachment. These nanocrystals have simpler shapes and well-defined crystal facets, and the chemical bonding strength of ligands is facet-specific. This results in reactive facets of one sort, and compelling atomically coherent “unified” crystals in one and two dimensions. In two dimensions, nanostructured single crystals emerge that have not only atomic order but also a second periodic geometry on the nanoscale; for instance, a 2D sheet with a square array of nanovoids or a honeycomb structure, with a geometry similar to that in silicene. It is clear that once scientists are able to master the nanocrystals’ shapes, ligand chemistry of the different facets, self-assembly into ordered reversible superstructures, and, finally, the atomic motion by which crystalline necks are formed and a single crystal emerges, nanocrystal assembly and oriented attachment



will become a strong engineering tool for crystalline materials with concomitant atomic and nanoperic order, of large interest in catalysis, in optoelectronics and for materials in the quantum age.

## ■ ASSOCIATED CONTENT

### SI Supporting Information

The Supporting Information is available free of charge at <https://pubs.acs.org/doi/10.1021/acs.accounts.0c00739>.

Short overview of oriented attachment in aqueous solvents as an alternative crystal growth process; tabulated overview of reports on oriented attachment of charge-stabilized crystals in polar solvents; tabulated overview of reports on oriented attachment in organic nonpolar solvents (PDF)

## ■ AUTHOR INFORMATION

### Corresponding Author

**Daniel Vanmaekelbergh** – Condensed Matter and Interfaces, Debye Institute for Nanomaterials Science, Utrecht University, 3508 TA Utrecht, The Netherlands; [orcid.org/0000-0002-3535-8366](https://orcid.org/0000-0002-3535-8366); Email: [d.vanmaekelbergh@uu.nl](mailto:d.vanmaekelbergh@uu.nl)

### Authors

**Bastiaan B. V. Salzmans** – Condensed Matter and Interfaces, Debye Institute for Nanomaterials Science, Utrecht University, 3508 TA Utrecht, The Netherlands; [orcid.org/0000-0002-8055-4681](https://orcid.org/0000-0002-8055-4681)

**Maaïke M. van der Sluijs** – Condensed Matter and Interfaces, Debye Institute for Nanomaterials Science, Utrecht University, 3508 TA Utrecht, The Netherlands; [orcid.org/0000-0001-7097-5506](https://orcid.org/0000-0001-7097-5506)

**Giuseppe Soligno** – Condensed Matter and Interfaces, Debye Institute for Nanomaterials Science, Utrecht University, 3508 TA Utrecht, The Netherlands; [orcid.org/0000-0003-2360-2082](https://orcid.org/0000-0003-2360-2082)

Complete contact information is available at: <https://pubs.acs.org/doi/10.1021/acs.accounts.0c00739>

### Author Contributions

<sup>†</sup>B.B.V.S. and M.M.v.d.S. contributed equally to this work.

### Notes

The authors declare no competing financial interest.

### Biographies

**Bastiaan Salzmans** received his master's degree in Chemistry and Physics in 2017 from Utrecht University. He is currently a Ph.D. student in the research group of Daniel Vanmaekelbergh.

**Maaïke van der Sluijs** received her master's degree in Chemistry and Physics in 2017 from Utrecht University. She is currently a Ph.D. student in the research group of Daniel Vanmaekelbergh.

**Giuseppe Soligno** received his Ph.D. in the group of Theoretical Physics at Utrecht University on the nanocrystal adsorption at liquid–air interfaces. He is currently performing molecular dynamics simulations on the formation of two-dimensional platelets and superlattices.

**Daniel Vanmaekelbergh** is senior research leader of the Group Condensed Matter and Interfaces at Utrecht University and director of the Debye Institute for Nanomaterials Science. He received an

ERC Advanced Grant on the formation of honeycomb semiconductors by nanocrystal self-assembly in 2016. He is an honorary member of the Israel Chemical Society. He received the Descartes-Huygens Prize from the French Academy of Science in 2017.

## ■ ACKNOWLEDGMENTS

B.B.V.S. and D.V. acknowledge The Netherlands Organization for Scientific Research (NWO) TOP-grant with Project No. 715.016.002. D.V., G.S., and M.M.v.d.S. acknowledge the ERC Advanced Grant “First Step” No. 692691.

## ■ ABBREVIATIONS

EG, ethylene glycol; GIWAXS, grazing incidence wide-angle X-ray scattering; MD, molecular dynamics; MSC, magic size cluster; NC, nanocrystal; SAED, selected area electron diffraction; SAXS, small-angle X-ray scattering; TEM, transmission electron microscopy

## ■ REFERENCES

- (1) Boneschanscher, M. P.; Evers, W. H.; Geuchies, J. J.; Altantzis, T.; Goris, B.; Rabouw, F. T.; van Rossum, S. A.; van der Zant, H. S.; Siebbeles, L. D.; Van Tendeloo, G.; Swart, I.; Hilhorst, J.; Petukhov, A. V.; Bals, S.; Vanmaekelbergh, D. Long-range orientation and atomic attachment of nanocrystals in 2D honeycomb superlattices. *Science* **2014**, *344*, 1377–1380.
- (2) Geuchies, J. J.; van Overbeek, C.; Evers, W. H.; Goris, B.; de Backer, A.; Gantapara, A. P.; Rabouw, F. T.; Hilhorst, J.; Peters, J. L.; Kononov, O.; Petukhov, A. V.; Dijkstra, M.; Siebbeles, L. D.; van Aert, S.; Bals, S.; Vanmaekelbergh, D. In situ study of the formation mechanism of two-dimensional superlattices from PbSe nanocrystals. *Nat. Mater.* **2016**, *15*, 1248–1254.
- (3) Peters, J. L.; Altantzis, T.; Lobato, I.; Jazi, M. A.; van Overbeek, C.; Bals, S.; Vanmaekelbergh, D.; Sinai, S. B. Mono- and Multilayer Silicene-Type Honeycomb Lattices by Oriented Attachment of PbSe Nanocrystals: Synthesis, Structural Characterization, and Analysis of the Disorder. *Chem. Mater.* **2018**, *30*, 4831–4837.
- (4) Verwey, E. J. W.; Overbeek, J. T. G. *Theory of stability of lyophobic colloids*; Dover: Mineola, NY, USA, 1999.
- (5) Banfield, J. F.; Welch, S. A.; Zhang, H. Z.; Ebert, T. T.; Penn, R. L. Aggregation-based crystal growth and microstructure development in natural iron oxyhydroxide biomineralization products. *Science* **2000**, *289*, 751–754.
- (6) Niederberger, M.; Colfen, H. Oriented attachment and mesocrystals: Non-classical crystallization mechanisms based on nanoparticle assembly. *Phys. Chem. Chem. Phys.* **2006**, *8*, 3271–3287.
- (7) De Yoreo, J. J.; Gilbert, P. U.; Sommerdijk, N. A.; Penn, R. L.; Whitlam, S.; Joester, D.; Zhang, H.; Rimer, J. D.; Navrotsky, A.; Banfield, J. F.; Wallace, A. F.; Michel, F. M.; Meldrum, F. C.; Colfen, H.; Dove, P. M. CRYSTAL GROWTH. Crystallization by particle attachment in synthetic, biogenic, and geologic environments. *Science* **2015**, *349*, No. aaa6760.
- (8) Murray, C. B.; Norris, D. J.; Bawendi, M. G. Synthesis and characterization of nearly monodisperse CdE (E = sulfur, selenium, tellurium) semiconductor nanocrystallites. *J. Am. Chem. Soc.* **1993**, *115*, 8706–8715.
- (9) Vanmaekelbergh, D. Self-assembly of colloidal nanocrystals as route to novel classes of nanostructured materials. *Nano Today* **2011**, *6*, 419–437.
- (10) Evers, W. H.; De Nijs, B.; Filion, L.; Castillo, S.; Dijkstra, M.; Vanmaekelbergh, D. Entropy-driven formation of binary semiconductor-nanocrystal superlattices. *Nano Lett.* **2010**, *10*, 4235–4241.
- (11) Bodnarchuk, M. I.; Kovalenko, M. V.; Heiss, W.; Talapin, D. V. Energetic and Entropic Contributions to Self-Assembly of Binary Nanocrystal Superlattices: Temperature as the Structure-Directing Factor. *J. Am. Chem. Soc.* **2010**, *132*, 11967–11977.

- (12) Drijvers, E.; De Roo, J.; Martins, J. C.; Infante, I.; Hens, Z. Ligand Displacement Exposes Binding Site Heterogeneity on CdSe Nanocrystal Surfaces. *Chem. Mater.* **2018**, *30*, 1178–1186.
- (13) Puzder, A.; Williamson, A. J.; Zaitseva, N.; Galli, G.; Manna, L.; Alivisatos, A. P. The effect of organic ligand binding on the growth of CdSe nanoparticles probed by Ab initio calculations. *Nano Lett.* **2004**, *4*, 2361–2365.
- (14) Yin, Y.; Alivisatos, A. P. Colloidal nanocrystal synthesis and the organic-inorganic interface. *Nature* **2005**, *437*, 664–670.
- (15) Cho, K. S.; Talapin, D. V.; Gaschler, W.; Murray, C. B. Designing PbSe nanowires and nanorings through oriented attachment of nanoparticles. *J. Am. Chem. Soc.* **2005**, *127*, 7140–7147.
- (16) Schliehe, C.; Juarez, B. H.; Pelletier, M.; Jander, S.; Greshnykh, D.; Nagel, M.; Meyer, A.; Foerster, S.; Kornowski, A.; Klinke, C.; Weller, H. Ultrathin PbS sheets by two-dimensional oriented attachment. *Science* **2010**, *329*, 550–3.
- (17) Brennan, J. G.; Siegrist, T.; Carroll, P. J.; Stuczynski, S. M.; Brus, L. E.; Steigerwald, M. L. The preparation of large semiconductor clusters via the pyrolysis of a molecular precursor. *J. Am. Chem. Soc.* **1989**, *111*, 4141–3.
- (18) Steigerwald, M. L.; Brus, L. E. Synthesis, stabilization, and electronic structure of quantum semiconductor nanoclusters. *Annu. Rev. Mater. Sci.* **1989**, *19*, 471–95.
- (19) Talapin, D. V.; Shevchenko, E. V. Introduction: Nanoparticle Chemistry. *Chem. Rev.* **2016**, *116*, 10343–10345.
- (20) Talapin, D. V.; Steckel, J. Quantum dot light-emitting devices. *MRS Bull.* **2013**, *38*, 685–695.
- (21) Kovalenko, M. V.; Manna, L.; Cabot, A.; Hens, Z.; Talapin, D. V.; Kagan, C. R.; Klimov, V. I.; Rogach, A. L.; Reiss, P.; Milliron, D. J.; Guyot-Sionnest, P.; Konstantatos, G.; Parak, W. J.; Hyeon, T.; Korgel, B. A.; Murray, C. B.; Heiss, W. Prospects of nanoscience with nanocrystals. *ACS Nano* **2015**, *9*, 1012–57.
- (22) Lim, J.; Park, Y. S.; Wu, K. F.; Yun, H. J.; Klimov, V. I. Droop-Free Colloidal Quantum Dot Light-Emitting Diodes. *Nano Lett.* **2018**, *18*, 6645–6653.
- (23) Erickson, C. S.; Bradshaw, L. R.; McDowall, S.; Gilbertson, J. D.; Gamelin, D. R.; Patrick, D. L. Zero-Reabsorption Doped-Nanocrystal Luminescent Solar Concentrators. *ACS Nano* **2014**, *8*, 3461–3467.
- (24) Frecker, T.; Bailey, D.; Arzeta-Ferrer, X.; McBride, J.; Rosenthal, S. J. Review-Quantum Dots and Their Application in Lighting, Displays, and Biology. *ECS J. Solid State Sci. Technol.* **2016**, *5*, R3019–R3031.
- (25) Araujo, J. J.; Brozek, C. K.; Kroupa, D.; Gamelin, D. R. Degenerately n-Doped Colloidal PbSe Quantum Dots: Band Assignments and Electrostatic Effects. *Nano Lett.* **2018**, *18*, 3893–3900.
- (26) Swart, I.; Liljeroth, P.; Vanmaekelbergh, D. Scanning probe microscopy and spectroscopy of colloidal semiconductor nanocrystals and assembled structures. *Chem. Rev.* **2016**, *116*, 11181–11219.
- (27) Peters, J. L.; van den Bos, K. H. W.; Van Aert, S.; Goris, B.; Bals, S.; Vanmaekelbergh, D. Ligand-Induced Shape Transformation of PbSe Nanocrystals. *Chem. Mater.* **2017**, *29*, 4122–4128.
- (28) Murray, C. B.; Kagan, C. R.; Bawendi, M. G. Self-Organization of CdSe Nanocrystallites into Three-Dimensional Quantum Dot Superlattices. *Science* **1995**, *270*, 1335–1338.
- (29) Rosenberg, R.; Murray, C. B. From materials to devices: Scaling and integration. *Annu. Rev. Mater. Sci.* **2000**, *30*, XII–XV.
- (30) Boles, M. A.; Engel, M.; Talapin, D. V. Self-Assembly of Colloidal Nanocrystals: From Intricate Structures to Functional Materials. *Chem. Rev.* **2016**, *116*, 11220–89.
- (31) Bian, K.; Choi, J. J.; Kaushik, A.; Clancy, P.; Smilgies, D. M.; Hanrath, T. Shape-anisotropy driven symmetry transformations in nanocrystal superlattice polymorphs. *ACS Nano* **2011**, *5*, 2815–23.
- (32) Choi, J. J.; Bealing, C. R.; Bian, K.; Hughes, K. J.; Zhang, W.; Smilgies, D. M.; Hennig, R. G.; Engstrom, J. R.; Hanrath, T. Controlling nanocrystal superlattice symmetry and shape-anisotropic interactions through variable ligand surface coverage. *J. Am. Chem. Soc.* **2011**, *133*, 3131–8.
- (33) Roest, A. L.; Houtepen, A. J.; Kelly, J. J.; Vanmaekelbergh, D. Electron-conducting quantum-dot solids with ionic charge compensation. *Faraday Discuss.* **2004**, *125*, 55–62.
- (34) Chandler, R. E.; Houtepen, A. J.; Nelson, J.; Vanmaekelbergh, D. Electron transport in quantum dot solids: Monte Carlo simulations of the effects of shell filling, Coulomb repulsions, and site disorder. *Phys. Rev. B: Condens. Matter Mater. Phys.* **2007**, *75*, 085325.
- (35) Houtepen, A. J.; Kockmann, D.; Vanmaekelbergh, D. Reappraisal of Variable-Range Hopping in Quantum-Dot Solids. *Nano Lett.* **2008**, *8*, 3516.
- (36) Lee, J.-S.; Kovalenko, M. V.; Huang, J.; Chung, D. S.; Talapin, D. V. Band-like transport, high electron mobility and high photoconductivity in all-inorganic nanocrystal arrays. *Nat. Nanotechnol.* **2011**, *6*, 348–352.
- (37) Woo, J. Y.; Ko, J. H.; Song, J. H.; Kim, K.; Choi, H.; Kim, Y. H.; Lee, D. C.; Jeong, S. Ultrastable PbSe nanocrystal quantum dots via in situ formation of atomically thin halide adlayers on PbSe(100). *J. Am. Chem. Soc.* **2014**, *136*, 8883–6.
- (38) Baumgardner, W. J.; Whitham, K.; Hanrath, T. Confined-but-connected quantum solids via controlled ligand displacement. *Nano Lett.* **2013**, *13*, 3225–31.
- (39) Grimaldi, G.; van den Brom, M. J.; du Fossé, I.; Crisp, R. W.; Kirkwood, N.; Gudjonsdottir, S.; Geuchies, J. J.; Kinge, S.; Siebbeles, L. D. A.; Houtepen, A. J. Engineering the Band Alignment in QD Heterojunction Films via Ligand Exchange. *J. Phys. Chem. C* **2019**, *123*, 29599–29608.
- (40) Yu, D.; Wang, C. J.; Guyot-Sionnest, P. n-type conducting CdSe nanocrystal solids. *Science* **2003**, *300*, 1277–1280.
- (41) Lan, X. Z.; Chen, M. L.; Hudson, M. H.; Kamysbayev, V.; Wang, Y. Y.; Guyot-Sionnest, P.; Talapin, D. V. Quantum dot solids showing state-resolved band-like transport. *Nat. Mater.* **2020**, *19*, 323–329.
- (42) Oh, S. J.; Wang, Z.; Berry, N. E.; Choi, J.-H.; Zhao, T.; Gauding, E. A.; Paik, T.; Lai, Y.; Murray, C. B.; Kagan, C. R. Engineering Charge Injection and Charge Transport for High Performance PbSe Nanocrystal Thin Film Devices and Circuits. *Nano Lett.* **2014**, *14*, 6210–6216.
- (43) Evers, W. H.; Goris, B.; Bals, S.; Casavola, M.; de Graaf, J.; van Rooij, R.; Dijkstra, M.; Vanmaekelbergh, D. Low-dimensional semiconductor superlattices formed by geometric control over nanocrystal attachment. *Nano Lett.* **2013**, *13*, 2317–23.
- (44) Sandeep, C. S. S.; Azpiroz, J. M.; Evers, W. H.; Boehme, S.-C.; Moreels, I.; Kinge, S.; Siebbeles, L. D. A.; Infante, I.; Houtepen, A. J. Epitaxially Connected PbSe Quantum-Dot Films: Controlled Neck Formation and Optoelectronic Properties. *ACS Nano* **2014**, *8*, 11499–11511.
- (45) van Overbeek, C.; Peters, J. L.; van Rossum, S. A. P.; Smits, M.; van Huis, M. A.; Vanmaekelbergh, D. Interfacial Self-Assembly and Oriented Attachment in the Family of PbX (X = S, Se, Te) Nanocrystals. *J. Phys. Chem. C* **2018**, *122*, 12464–12473.
- (46) Kalesaki, E.; Delerue, C.; Morais Smith, C.; Beugeling, W.; Allan, G.; Vanmaekelbergh, D. Dirac Cones, Topological Edge States, and Nontrivial Flat Bands in Two-Dimensional Semiconductors with a Honeycomb Nanogeometry. *Phys. Rev. X* **2014**, *4*, 011010.
- (47) Beugeling, W.; Kalesaki, E.; Delerue, C.; Niquet, Y. M.; Vanmaekelbergh, D.; Morais Smith, C. Topological states in multi-orbital HgTe honeycomb lattices. *Nat. Commun.* **2015**, *6*, 6316.
- (48) Evers, W. H.; Schins, J. M.; Aerts, M.; Kulkarni, A.; Capiod, P.; Berthe, M.; Grandidier, B.; Delerue, C.; van der Zant, H. S. J.; van Overbeek, C.; Peters, J. L.; Vanmaekelbergh, D.; Siebbeles, L. D. A. High charge mobility in two-dimensional percolative networks of PbSe quantum dots connected by atomic bonds. *Nat. Commun.* **2015**, *6*, 8195.
- (49) Alimoradi Jazi, M.; Janssen, V.; Evers, W. H.; Tadjine, A.; Delerue, C.; Siebbeles, L. D. A.; van der Zant, H. S. J.; Houtepen, A. J.; Vanmaekelbergh, D. Transport Properties of a Two-Dimensional PbSe Square Superstructure in an Electrolyte-Gated Transistor. *Nano Lett.* **2017**, *17*, 5238–5243.



(50) Alimoradi Jazi, M.; Kulkarni, A.; Sinai, S. B.; Peters, J. L.; Geschiere, E.; Failla, M.; Delerue, C.; Houtepen, A. J.; Siebbeles, L. D. A.; Vanmaekelbergh, D. Room-Temperature Electron Transport in Self-Assembled Sheets of PbSe Nanocrystals with a Honeycomb Nanogeometry. *J. Phys. Chem. C* **2019**, *123*, 14058–14066.

(51) Tadjine, A.; Allan, G.; Delerue, C. From lattice Hamiltonians to tunable band structures by lithographic design. *Phys. Rev. B: Condens. Matter Mater. Phys.* **2016**, *94*, 075441.

(52) Walravens, W.; Solano, E.; Geenen, F.; Dendooven, J.; Gorobtsov, O.; Tadjine, A.; Mahmoud, N.; Ding, P. P.; Ruff, J. P. C.; Singer, A.; Roelkens, G.; Delerue, C.; Detavernier, C.; Hens, Z. Setting Carriers Free: Healing Faulty Interfaces Promotes Delocalization and Transport in Nanocrystal Solids. *ACS Nano* **2019**, *13*, 12774–12786.

(53) Delerue, C. Nanocrystal solids: Order and progress. *Nat. Mater.* **2016**, *15*, 498–499.

(54) Koh, W. K.; Bartnik, A. C.; Wise, F. W.; Murray, C. B. Synthesis of monodisperse PbSe nanorods: a case for oriented attachment. *J. Am. Chem. Soc.* **2010**, *132*, 3909–13.

(55) Ramin Moayed, M. M.; Li, F.; Beck, B.; Schober, J. C.; Klinke, C. Anisotropic circular photogalvanic effect in colloidal tin sulfide nanosheets. *Nanoscale* **2020**, *12*, 6256–6262.

(56) Klokkenburg, M.; Houtepen, A. J.; Koole, R.; de Folter, J. W. J.; Erne, B. H.; van Faassen, E.; Vanmaekelbergh, D. Dipolar structures in colloidal dispersions of PbSe and CdSe quantum dots. *Nano Lett.* **2007**, *7*, 2931–2936.

(57) Schapotschnikow, P.; van Huis, M. A.; Zandbergen, H. W.; Vanmaekelbergh, D.; Vlugt, T. J. H. Morphological Transformations and Fusion of PbSe Nanocrystals Studied Using Atomistic Simulations. *Nano Lett.* **2010**, *10*, 3966–3971.

(58) Fang, C.; van Huis, M. A.; Vanmaekelbergh, D.; Zandbergen, H. W. Energetics of polar and nonpolar facets of PbSe nanocrystals from theory and experiment. *ACS Nano* **2010**, *4*, 211–8.

(59) Walravens, W.; De Roo, J.; Drijvers, E.; Ten Brinck, S.; Solano, E.; Dendooven, J.; Detavernier, C.; Infante, I.; Hens, Z. Chemically Triggered Formation of Two-Dimensional Epitaxial Quantum Dot Superlattices. *ACS Nano* **2016**, *10*, 6861–70.

(60) Soligno, G.; Dijkstra, M.; van Rooij, R. Self-Assembly of Cubes into 2D Hexagonal and Honeycomb Lattices by Hexapolar Capillary Interactions. *Phys. Rev. Lett.* **2016**, *116*, 258001.

(61) Soligno, G.; Dijkstra, M.; van Rooij, R. Self-assembly of cubic colloidal particles at fluid-fluid interfaces by hexapolar capillary interactions. *Soft Matter* **2018**, *14*, 42–60.

(62) Soligno, G.; Vanmaekelbergh, D. Understanding the Formation of PbSe Honeycomb Superstructures by Dynamics Simulations. *Phys. Rev. X* **2019**, *9*, 021015.

(63) Soligno, G.; Vanmaekelbergh, D. Phase diagrams of honeycomb and square nanocrystal superlattices from the nanocrystal's surface chemistry at the dispersion-air interface. *J. Chem. Phys.* **2019**, *151*, 234702.

(64) Gupta, U.; Escobedo, F. A. Implicit solvent model for the interfacial configuration of colloidal nanoparticles and application to the self-assembly of truncated cubes. *J. Chem. Theory Comput.* **2020**, *16*, 5866–5875.

(65) Tang, Z.; Kotov, N. A.; Giersig, M. Spontaneous organization of single CdTe nanoparticles into luminescent nanowires. *Science* **2002**, *297*, 237–40.

(66) Pradhan, N.; Xu, H.; Peng, X. Colloidal CdSe quantum wires by oriented attachment. *Nano Lett.* **2006**, *6*, 720–4.

(67) Liu, X.; Wan, J.; Xiong, Y.; Liang, S.; Gao, Y.; Tang, Z. Synthesis of Uniform CdSe Quantum Wires via Oriented Attachment. *J. Nanosci. Nanotechnol.* **2015**, *15*, 5798–806.

(68) Ondry, J. C.; Philbin, J. P.; Lostica, M.; Rabani, E.; Alivisatos, A. P. Resilient Pathways to Atomic Attachment of Quantum Dot Dimers and Artificial Solids from Faceted CdSe Quantum Dot Building Blocks. *ACS Nano* **2019**, *13*, 12322–12344.

(69) Tang, Z.; Zhang, Z.; Wang, Y.; Glotzer, S. C.; Kotov, N. A. Self-assembly of CdTe nanocrystals into free-floating sheets. *Science* **2006**, *314*, 274–8.

(70) Wang, Y.; Peng, X.; Abelson, A.; Zhang, B.-K.; Qian, C.; Ercius, P.; Wang, L.-W.; Law, M.; Zheng, H. In situ TEM observation of neck formation during oriented attachment of PbSe nanocrystals. *Nano Res.* **2019**, *12*, 2549–2553.

(71) daSilva, J. C.; Smeaton, M. A.; Dunbar, T. A.; Xu, Y.; Balazs, D. M.; Kourkoutis, L. F.; Hanrath, T. Mechanistic Insights into Superlattice Transformation at a Single Nanocrystal Level Using Nanobeam Electron Diffraction. *Nano Lett.* **2020**, *20*, 5267–5274.

(72) Choi, J. J.; Bian, K.; Baumgardner, W. J.; Smilgies, D. M.; Hanrath, T. Interface-induced nucleation, orientational alignment and symmetry transformations in nanocube superlattices. *Nano Lett.* **2012**, *12*, 4791–8.

(73) Weidman, M. C.; Smilgies, D. M.; Tisdale, W. A. Kinetics of the self-assembly of nanocrystal superlattices measured by real-time in situ X-ray scattering. *Nat. Mater.* **2016**, *15*, 775–81.

(74) Geuchies, J. J.; Soligno, G.; Geraffy, E.; Hendrikx, C. P.; Overbeek, C. v.; Montanarella, F.; Slot, M. R.; Kononov, O. V.; Petukhov, A. V.; Vanmaekelbergh, D. Unravelling three-dimensional adsorption geometries of PbSe nanocrystal monolayers at a liquid-air interface. *Commun. Chem.* **2020**, *3*, 28.

(75) Afsar-Siddiqui, A. B.; Luckham, P. F.; Matar, O. K. The spreading of surfactant solutions on thin liquid films. *Adv. Colloid Interface Sci.* **2003**, *106*, 183–236.

(76) Balazs, D. M.; Dunbar, T. A.; Smilgies, D. M.; Hanrath, T. The coupled dynamics of colloidal nanoparticle spreading and self-assembly at a fluid-fluid interface. *Langmuir* **2020**, *36*, 6106–6115.

(77) Sushko, M. L. Understanding the driving forces for crystal growth by oriented attachment through theory and simulations. *J. Mater. Res.* **2019**, *34*, 2914–2927.

(78) Peters, J. L.; Soligno, G.; van der Sluijs, M. M.; Vanmaekelbergh, D., Structural reconfigurations and long-range order in 2-dimensional assemblies of attached PbSe nanocrystals. Manuscript in preparation.